JOURNAL OF ENGINEERING AND APPLIED SCIENCE, VOL. 51, NO. 2, APR. 2004, PP. 233-252
FACULTY OF ENGINEERING, CAIRO UNIVERSITY

DEVELOPMENT OF A TWO-PARAMETER SEISMIC INTENSITY MEASURE AND PROBABILISTIC DESIGN PROCEDURE

S. S. MEHANNY[1] AND P. P. CORDOVA[2]

ABSTRACT

A method to evaluate the seismic collapse performance of frame structures through a probability-based assessment procedure is presented, considering uncertainties in both the ground motion hazard and inelastic structural response to extreme input ground motions. The procedure includes a new seismic-intensity scaling index that accounts for period softening and thereby reduces the large record-to-record variability typically observed in inelastic time-history analyses. Equations are developed to combine results from inelastic time history analyses and a site-specific hazard curve to calculate the mean annual probability of a structure exceeding its collapse limit state.

KEYWORDS: Seismic intensity measure, collapse, frame structures, probability of failure, inelastic analysis, time history analysis.

1. INTRODUCTION

Research on performance-based earthquake engineering poses many challenges, among them being the need for a consistent methodology to predict structural collapse as a function of the earthquake ground motion intensity. Components to an assessment methodology for collapse should include (1) definition of the seismic hazard, (2) simulation of structural response to input ground motions, including stiffness and strength degradation, and (3) statistical interpretation of results. The methodology must rigorously account for variability in performance prediction due to uncertainties in the inherent seismic hazard and the nonlinear simulation of structural response.

[1] Assistant Professor, Structural Eng. Dept., Faculty of Engineering, Cairo University, Giza, EGYPT.
[2] Researcher, John A. Blume Earthquake Engineering Center, CA, USA.

A large source of variability in seismic performance assessment arises from simplifications in defining earthquake intensity relative to the true damaging effects of ground motions on structures. Current codes (e.g. [1]) define earthquake hazard in terms of spectral response coefficients, typically spectral acceleration measured at the first mode period of vibration, $S_a(T_1)$. First mode spectral acceleration is the basis of equivalent lateral force design procedures, and it is often used as the default earthquake intensity scaling parameter for time-history analyses. While first mode spectral acceleration is an accurate index for structures that respond elastically, this single parameter does not reflect many of the aspects of earthquake ground motions that affect inelastic stiffness and strength degradation. An objective of this paper is to examine a new two-parameter hazard intensity index that can improve the accuracy of structural performance predictions based on inelastic time history analyses. A related objective is the development of reliability-based equations for interpreting the performance limit state to compare the effect of using a single versus two-parameter intensity measure.

The scope and approach of this paper is as follows. First, the general concepts of earthquake ground motion intensity measures are introduced, including an overview of traditional measures and the development of attenuation functions for the new proposed index. Second, a series of case study buildings are introduced to calibrate the new earthquake intensity measure. Next, a probability-based assessment procedure is developed to describe the collapse performance in terms of mean annual probability of exceedance and an equivalent load and resistance format. Finally, the probabilistic assessment procedure is demonstrated through an application to one of the case study buildings.

2. HAZARD INTENSITY MEASURES

Traditionally, building codes have quantified earthquake intensity as a function of either peak ground motions (acceleration or velocity) or linear response spectrum quantities (acceleration, velocity, or displacement). As implied by their name, linear

response spectrum quantities do a good job at characterizing earthquake effects in structures that respond elastically, but they do not necessarily capture inelastic behavior. More elaborate indices, which seek to improve characterization of earthquake ground motions, have been the subject of continuing studies. For example, Housner [2] proposed combining spectral acceleration together with strong motion duration. More recently, Luco [3] has proposed extending linear spectral quantities into the nonlinear realm through the use of inelastic spectral response demands. While they are generally more accurate, one drawback of the nonlinear spectral values is that they imply a coupling between the earthquake hazard definition and the inelastic structural properties. This complicates development of seismic hazard maps for general use. Another topic of recent research concerns near fault directivity effects and whether these warrant specialized treatment in earthquake hazard characterization (e.g., [4]).

Common to most studies of improved intensity measures is the goal to characterize ground motion hazards in a statistically meaningful way for predicting structural performance. This implies that the best intensity measures are those that result in the least record-to-record variability, measured with respect to a common intensity index, when evaluating structural performance to multiple earthquake records. Of course, even with the best ground motion characterization, uncertainties will persist in characterizing the geologic earthquake hazard and in simulating inelastic structural performance.

2.1 Improved Hazard Intensity Measure - $S_a(T_1)R_{Sa}{}^{\alpha}$

The International Building Code [1] and most other earthquake engineering design standards in the United States define hazard intensity as the spectral acceleration of the ground motion, typically calculated at the fundamental (first mode) period of the structure. A known shortcoming of this measure is that it does not account for inelastic lengthening of the period as the structure softens under stiffness degradation. As illustrated in the response spectra plots of Fig. 1, two ground motions

characterized on the basis of their first-mode spectral response may result in significantly different inelastic response, depending on the slope of the spectra at lengthened periods. For example, when normalized with respect to $S_a(T_1)$, record #2 will inevitably produce larger inelastic deformations than record #1. This trend is not accounted for in the single spectral quantity, $S_a(T_1)$.

A simple extension to current practice that can help capture the period shift effect is to introduce a second intensity parameter that reflects spectral shape. The proposed parameter to do this is a ratio of spectral accelerations at two periods,

$$R_{S_a} = S_a(T_f) / S_a(T_1) \tag{1}$$

where T_1 is the first mode period and T_f is a longer period that represents the inelastic (damaged) structure. This ratio can then be combined with the first mode spectral acceleration, $S_a(T_1)$, to give the following new two-parameter hazard intensity measure

$$S^* = S_a(T_1) R_{S_a}{}^{\alpha} \tag{2}$$

where α and the ratio T_f/T_1 are determined by calibration to optimize the intensity index by minimizing the variability in computed results.

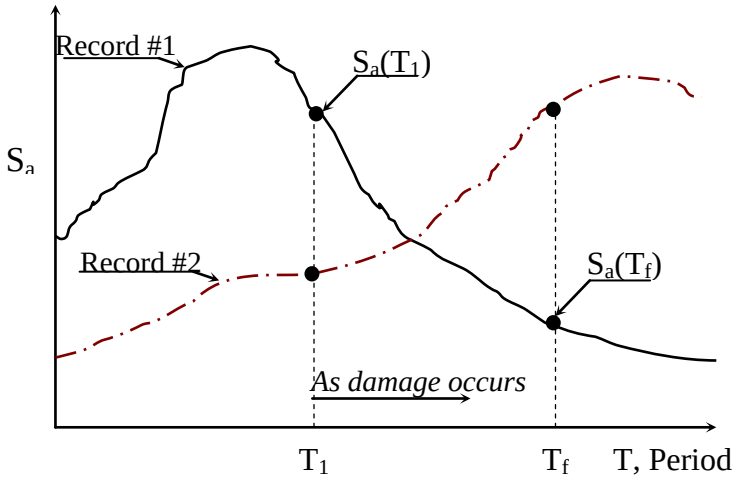

Fig. 1. Effects of structural softening.

2.2 Attenuation Functions for Two-Parameter Index

Given the prevalence of linear spectral acceleration in codes and practice, most hazard assessment techniques and data are geared toward predicting this quantity. For

example, national hazard maps available from USGS define earthquake hazard in terms of spectral acceleration at two periods (roughly *T = 0.2* second and *1* second) representative of short and long period structures. In devising new intensity measures, it is convenient if they can be derived by manipulating existing models and hazard data.

Since the proposed intensity measure, S^*, is simply a function of the spectral acceleration at two different periods (T_1 and T_f), it is relatively straightforward to modify existing attenuation function to accommodate this index. Eq. (3) shows the transformation of a single parameter attenuation function, $E[\ln S_a(T_x)]$, to the modified function, $E[\ln S^*]$, where $E[\ln \ldots]$ is read as the "expected value of the natural log of the given parameter" and other variables are as defined previously:

$$E\left[\ln S^*\right] = (1-\alpha)E\left[\ln S_a(T_1)\right] + \alpha E\left[\ln S_a(T_f)\right] \tag{3}$$

In addition to the expected value of *S**, the standard deviation, $\sigma_{\ln S^*}$, must also be defined. This in turn requires the correlation between spectral accelerations at the two periods, $S_a(T_1)$ and $S_a(T_f)$. Inoue [5] provides the following empirical correlation coefficient, $\rho_{\ln Sa_1 \ln Sa_f}$, that fills this need:

$$\rho_{\ln Sa_1 \ln Sa_f} = 1 - 0.33\left|\ln(1/T_1) - \ln(1/T_f)\right| \tag{4}$$

Given this correlation expression, the standard deviation of *S** can be defined as follows:

$$\sigma^2_{\ln S^*} = (1-\alpha)^2 \sigma^2_{\ln Sa_1} + \alpha^2 \sigma^2_{\ln Sa_f} + 2\rho_{\ln Sa_1 \ln Sa_f}(1-\alpha)\alpha\sigma_{\ln Sa_1}\sigma_{\ln Sa_f} \tag{5}$$

Most spectral attenuation relationships define empirical coefficients as a function of frequency or period that can be manipulated to calculate S* according to Eq. (3). For example, Abrahamson & Silva [6] define an attenuation function as follows:

$$E[\ln S_a] = a_1 + a_4(m-m_1) + a_{12}(8.5-m)^n + [a_3 + a_{13}(m-m_1)]\ln(R) \tag{6}$$

where the *a*-coefficients are tabulated [6], *m* is the earthquake magnitude, m_1 is a given base magnitude, and *R* is the distance from the epicenter to the site. Substituting Eq. (6) into Eq. (3), one obtains the following relationship for modified coefficients that can be applied in the otherwise standard attenuation relationship to obtain *S*:*

$$a_x^* = (1-\alpha)a_{xT1} + \alpha a_{xT2} \quad (7)$$

These relationships can then be applied in a standard probabilistic site hazard analysis where the required performance is evaluated on the basis of this new intensity, *S**.

3. BUILDING TESTBEDS

In related research [7] several moment frame structures have been developed and analyzed to exercise seismic assessment and design provisions for composite construction. These frames are utilized here to provide the basis for calibrating the new intensity measure parameters, α and T_f/T_1, and illustrate their application in a probabilistic performance assessment. The case study structures consist of three six-story frames and one twelve-story frame, all of which are designed according to provisions of the IBC [1] for a site in a high seismic region in California.

Three of the case study structures are composite moment frames composed of reinforced concrete columns and steel beams (referred to as RCS systems), and the forth is a steel space frame. An elevation of one of the frames, a six-story RCS perimeter frame, is shown in Fig. 2. As summarized in Table 1, vibration periods for the frames range from T_1 = 1.3 to 2.1 seconds. Please refer to [7] for more details.

Table 1. Tested frame data.

Frame ID	First Mode Period T_1 (sec)	IDA Dispersion Data for Alternative Intensity Measures					
		General Records			Near Fault Records		
		$\sigma_{\ln(IDR\|Sa)}$	$\sigma_{\ln(IDR\|SaRsa)}$ (Optimized)	$\sigma_{\ln(IDR\|SaRsa)}$ *(2.0,0.5)*	$\sigma_{\ln(IDR\|Sa)}$	$\sigma_{\ln(IDR\|SaRsa)}$ (Optimized)	$\sigma_{\ln(IDR\|SaRsa)}$ *(2.0,0.5)*
6S_RCS_S	1.3	0.42	0.28 *(1.9,0.65)*	0.29	0.45	0.22 *(1.8,0.9)*	0.27
6S_S_S	1.3	0.27	0.20 *(1.2,2.4)*	0.23	0.30	0.18 *(1.6,0.8)*	0.19
12S_RCS_S	2.1	0.24	0.19 *(1.6,0.6)*	0.22	0.26	0.21 *(2.4,0.4)*	0.22
6S_RCS_P	1.5	0.30	0.23 *(1.65,0.45)*	0.24	-	-	-

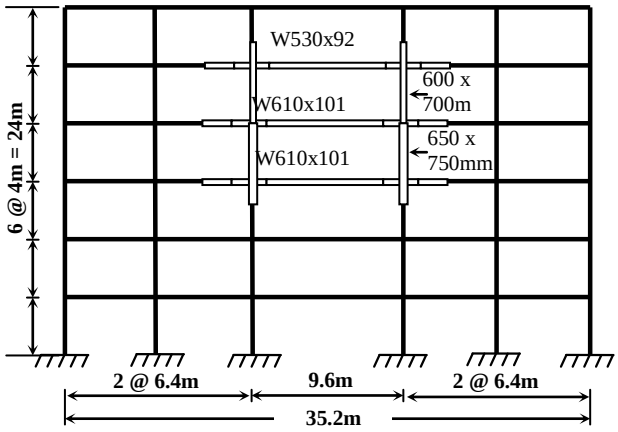

Fig. 2. Elevation of RCS perimeter frame.

Inelastic static and dynamic (time history) analyses are conducted using an analysis program [8] that takes into account second-order geometric behavior and spread-of-plasticity effects in the beam-columns and connections. Inelastic time history analyses are run simultaneously with gravity loads equal to 100% dead load and 25% live load.

4. COLLAPSE ANALYSIS TECHNIQUES

4.1 Incremented Dynamic Analysis

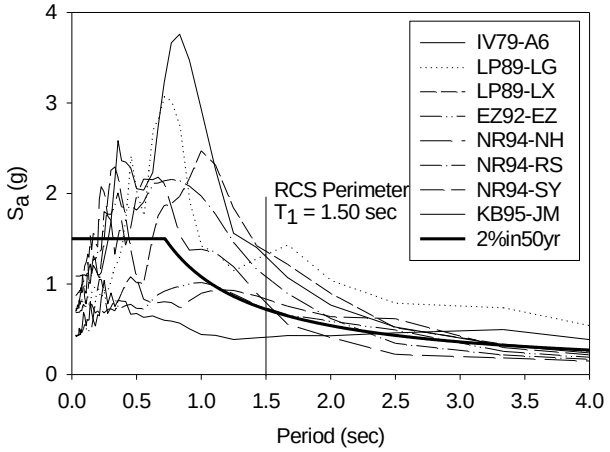

Fig. 3. Near Fault Response Spectrum.

Seismic performance is assessed through nonlinear time history analyses using two sets of ground motions – one comprised of eight general records and another of eight near-fault records with forward directivity [7]. Response spectra for the near-fault

records are superimposed on the 2% in 50-year design hazard spectrum used to design the case study buildings in Fig. 3. Acceleration components of the records are scaled, where the resulting ground motion intensity is reported in terms of either spectral acceleration, $S_a(T_1)$, or the proposed new index, $S_a R_{S_a}{}^{\alpha}$. Shome and Cornell [9] have demonstrated that such scaling of records will not bias the results and is an appropriate technique for multi-level hazard analysis.

Results of the time history analyses are summarized by plotting the scaled intensity measure versus maximum Interstory Drift Ratio (IDR), creating what are referred to herein as Incremented Dynamic Analysis (IDA) curves. Shown in Fig. 4 are examples of the IDA curves for the RCS perimeter frame building (6S_RCS_P) subjected to the general records, where each data point corresponds to the peak IDR resulting from a single time history analysis. The collection of data points for a single ground record scaled to multiple hazard levels forms the IDA curve. Results are plotted in terms of the $S_a(T_1)$ intensity in Fig. 4a and $S_a R_{S_a}{}^{\alpha}$ in Fig. 4b.

Comparing the graphs in Fig. 4, it is obvious that the two-parameter intensity measure (Fig. 4b) results in significantly less record-to-record variability than $S_a(T_1)$ (Fig. 4a). The variability can be quantified in terms of dispersion of the drift response conditioned on the ground motion intensity measure. Dispersion is calculated according to the following equation as the mean squared deviation of the drift data from an average response curve obtained by linear regression in log-log space between drift and the seismic intensity (of the form, $\ln \mathrm{IDR}_{\mathrm{MAX}} = A + B \ln \mathrm{IM}$):

$$\sigma_{\ln IDR_{MAX}|intensitymeasure} = \left[\sum_{i=1}^{n} (\ln IDR_{MAX,i} - \ln \hat{IDR}_{MAX})^2 / (n-1)\right]^{0.5} \qquad (8)$$

where $IDR_{MAX,i}$ is the ith response calculated for a given intensity, $\hat{IDR}_{MAX}$ is the value from the regression curve, and n is the total number of observations ($n=8$ in this case). Comparing Figs. 4a and 4b, the dispersion $\sigma_{ln(IDR,Sa)}$ = 0.30 for the $S_a(T_1)$ index is roughly 30% larger than that of $\sigma_{ln(IDR,SaR)}$ = 0.23 for $S_a R_{S_a}{}^{\alpha}$. This result is based on using the optimized coefficients of $\alpha=0.45$ and $T_f/T_1 = 1.65$ for the $S_a R_{S_a}{}^{\alpha}$ index,

determined by varying these factors so as to minimize the dispersion. Note that these optimal values are specific to 6S_RCS_P frame under the set of eight ground motions.

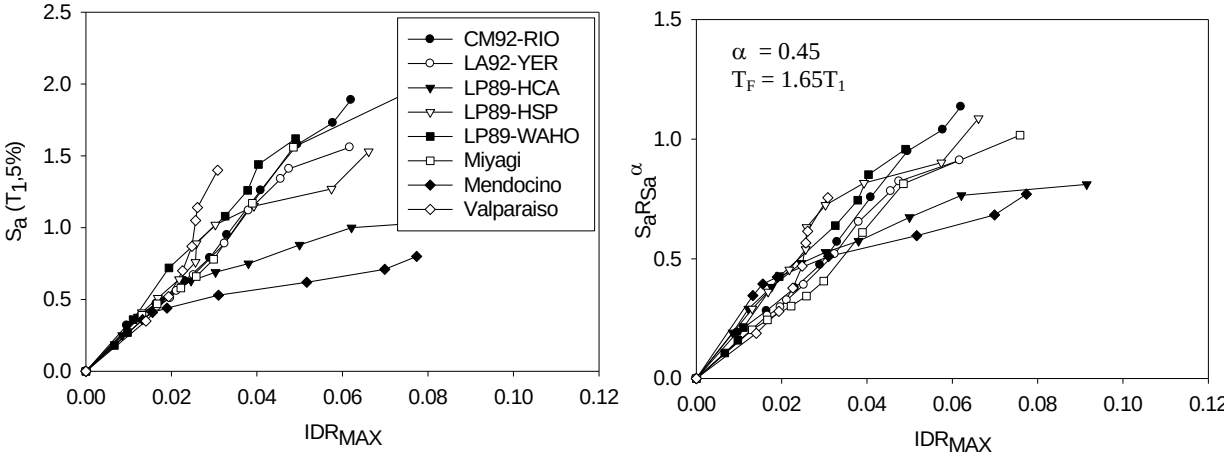

Fig. 4. IDA plots for 6S_RCS_P Frame: (a) IDR vs. $S_a(T_1)$ (b) IDR vs. $S_aR_{sa}{}^{\alpha}$.

While the two-parameter index reduces the overall dispersion, this reduction is most apparent at larger drifts, where the structure behaves nonlinearly. In fact, comparing Figs. 4a and 4b, in the elastic range (at lower drifts), the two-parameter $S_aR_{S_a}{}^{\alpha}$ index results in more variability than *Sa(T1).* This follows from the fact that *Sa(T1)* provides a nearly exact correlation with drift for the linear case, whereas the period shift captured in $S_aR_{S_a}{}^{\alpha}$ works best when the structure behaves nonlinearly. This suggests that an improved index would be one where the α and T_f parameters are devised to vary with the degree of inelastic action, similar in some ways to how the period is shifted using the capacity spectrum method for calculating the target displacement for nonlinear static pushover analyses.

4.2 Frame Stability Limit State Determination

To evaluate global instability, the authors have employed a procedure that integrates local damage indices, computed during the time-history analysis, through a supplementary stability analysis of the damaged structure [7]. The basic procedure entails a post-earthquake second-order inelastic stability analysis to assess the loss of

gravity load capacity due to damage incurred during the earthquake. This procedure leads to the plot of an intensity measure versus gravity stability index λ_u shown in Fig. 5. λ_u is defined as the ratio of the vertical load capacity to the applied gravity loads, where the gravity loads are assumed as full dead load plus 25% of the live load.

The stability index, λ_u, provides a global failure criterion that integrates the effect of local damage sustained under each earthquake record and intensity. The point where the curves cross $\lambda_u=1.0$ is point at which the structure can no longer sustain stability under its self-weight due to extensive seismic damage. The stability index at this point is defined as λ_f and the associated median value of the seismic hazard value is $\hat{\mu}_{\lambda_f}$. This level is defined as the 'capacity' – or collapse limit state – of the structure. Another limit point is identified at $\lambda_u = 0.95\lambda_{uo}$ where λ_{uo} is the initial value of λ_u for the undamaged (i.e., intact) structure. This point defines the sharp transition in the $S_a(T_1)$ or $S_a R_{S_a}{}^{\alpha}$ versus λ_u stability curve, representing the intensity level beyond which the stability index degrades rapidly.

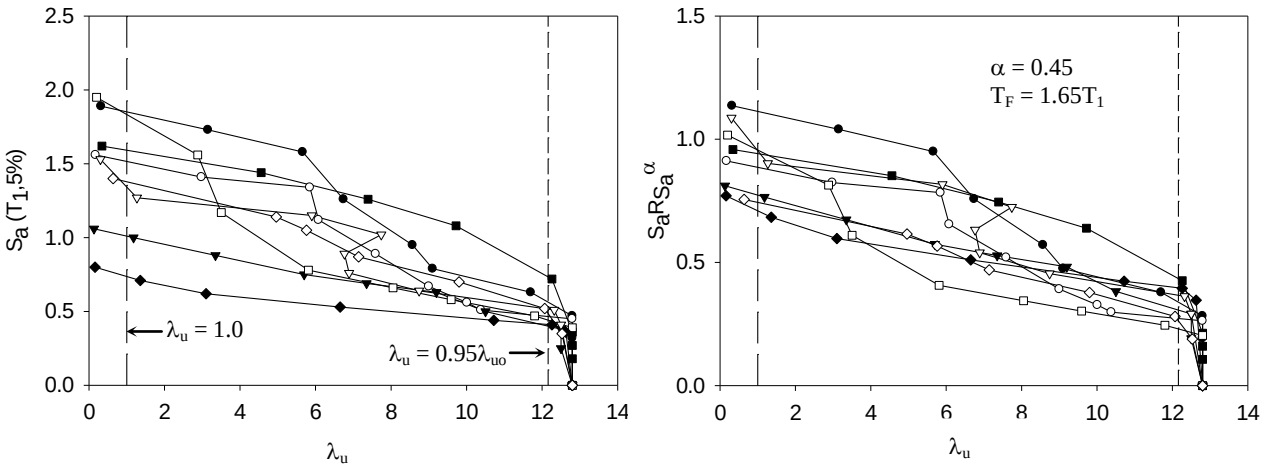

(a) (b)

Fig. 5. Stability curves versus IM, (a) IM = S_a, (b) IM = $S_a R_{sa}{}^{\alpha}$.

Similar to the IDA plots (Fig. 4), the $S_a(T_1)$ index shows much larger record-to-record variability in the λ_u response than the $S_a R_{S_a}{}^{\alpha}$ index. The standard deviations of $S_a(T_1)$ at $0.95\lambda_{uo}$ and λ_f are equal to 0.40 and 0.49, respectively, compared to 0.26 and 0.15

using $S_a R_{S_a}{}^{\alpha}$. This reduced variability leads to a better approximation of the expected collapse performance.

5. DETERMINATION OF GENERAL α AND T_f

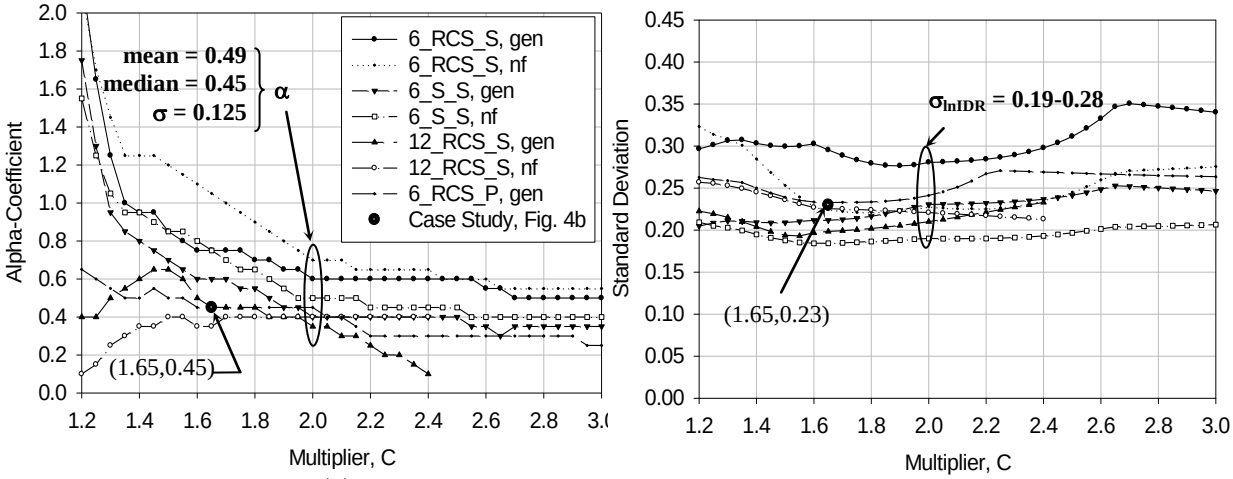

(a) (b)

Fig. 6. Optimization of $S_a R_{Sa}{}^{\alpha}$,
(a) Range of optimum α-C pairs and (b) Dispersion on α-C pairs.

The examples described above show how the proposed intensity measure, $S_a R_{S_a}{}^{\alpha}$, can significantly reduce the record-to-record variability in calculating the seismic performance. What remains to determine is optimum values of α and the period multiplier, $C=T_f/T_1$, which minimize dispersion for a broad class of building frames.

To determine the optimal calibration for α and *C*, IDA and λ_u stability analyses are run for each of the four structures under the sixteen ground motions (eight general and eight near fault). Next, the $S_a R_{S_a}{}^{\alpha}$ response data is plotted for various combinations of α and *C*, the average response curve is fit to the data, and the dispersion is calculated. This results in many α and *C* pairs for each structure, each with its own dispersion, σ_{lnIDR}. The optimal α and *C* pair for each structure is one that yields the least dispersion. The graphs in Fig. 6 show the resulting relationships between α, *C*, and the resulting dispersion for each structure and bin of ground motions. The

optimum alpha-coefficient is plotted versus the corresponding *C* in Fig. 6a, and the associated dispersions for the corresponding pairs of α and *C* are plotted in Fig. 6b.

Determination of one general pair of α and *C* obviously compromises the preciseness that can be achieved with multiple pairs tailored for each structure and each ground record. Nevertheless, a common calibration is desired to make the procedure convenient for generalized use. Referring to Fig. 6b, on average the dispersion turns out to be relatively constant over a large range of *C* and α pairs. Further, from Fig. 6a we see that the optimal α (given *C*) is relatively stable for $2 < C < 3$. This indicates that the intensity measure is somewhat insensitive, within a certain range, to the choice of period multiplier. Based on these observations, a pair of $C = 2.0$ ($T_f = 2.0T_1$) and $\alpha = 0.5$ is proposed for general use. Thus, the proposed intensity measure is:

$$S^* = S_a(T_1)\left[S_a(2.0T_1)/S_a(T_1)\right]^{0.5} = S_a R_{S_a}{}^{0.5} \tag{9}$$

Based on this definition, the data in Figs. 4b and 5b are re-plotted and shown in Fig. 7. Dispersion data for all three intensity measures ($S_a(T_1)$, the optimal $S_a R_{S_a}{}^{\alpha}$, and the generalized $S_a R_{S_a}{}^{0.5}$) are summarized for each frame in Table 1.

Referring to Table 1, in all cases the proposed intensity measure $(S_a R_{Sa}{}^{\alpha})$ consistently reduces the variability in the calculated structural response, compared to the $S_a(T_1)$ index. The two-parameter index with optimum coefficients $(S_a R_{Sa}{}^{\alpha})$ obviously does a better job than the average index ($S_a R_{Sa}{}^{0.5}$ per Eq. 9), but the average index still does well – particularly where the dispersion is large for the original $S_a(T_1)$ index. Conversely, the only cases where the new index fails to make a significant impact is those instances where the variability of the response is already low when scaled by spectral acceleration alone. Comparing results for the average two-parameter index (Eq. 9) with $S_a(T_1)$, the two-parameter index reduces the range of dispersion from 0.24-0.45 for $S_a(T_1)$ to 0.19-0.29 for $S_a R_{Sa}{}^{0.5}$.

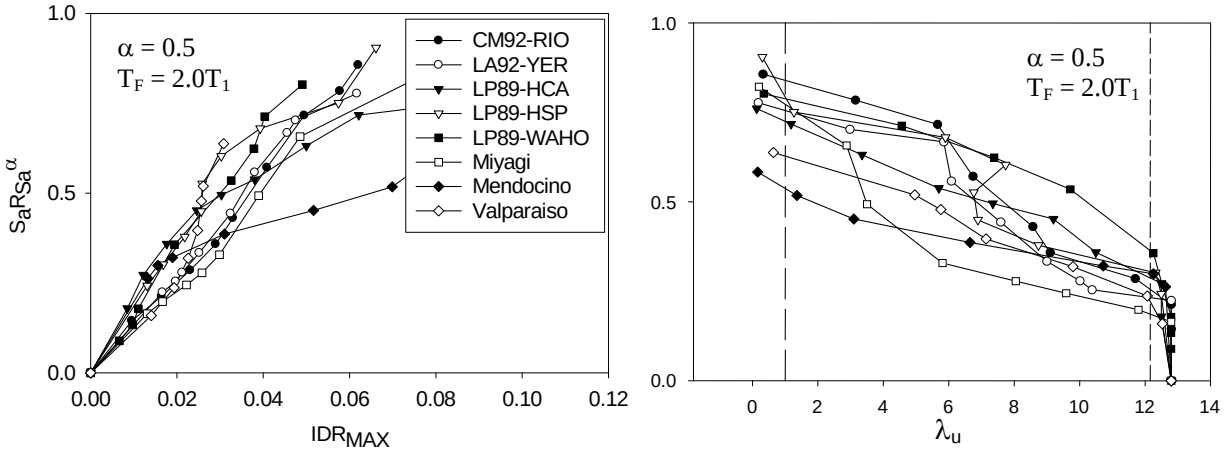

Fig. 7. Updated Behavior Curves with IM = $S_aR_{Sa}^{0.5}$
(a) IDA and (b) stability curves.

6. PROBABILITY ASSESSMENT OF COLLAPSE PREVENTION

Using the inelastic time-history and stability analysis method described above, the "collapse prevention" performance for a given set of ground motion records is defined by the stability limit, $\hat{\mu}_{\lambda_f}$, defined in terms of the seismic hazard intensity – either $S_a(T_1)$ or $S_aR_{Sa}^{0.5}$. The next step in the performance assessment is to compare the stability limit to the seismic hazard, considering the uncertainty in both the calculated response indices and the site hazard curve.

6.1 Mean Annual Probability of Exceedance

Defining failure (collapse) by the likelihood of the ground motion intensity exceeding the stability limit $\hat{\mu}_{\lambda_f}$ the mean annual probability of collapse can be described by:

$$P_f = P\left[IM \geq \hat{\mu}_{\lambda_f}\right] \tag{10}$$

where P_f is the mean annual probability of failure and *IM* is the seismic hazard demand expressed using an intensity measure consistent with that used to define the stability limit, $\hat{\mu}_{\lambda_f}$. In this case, the two alternative intensity measures considered are $S_a(T_1)$ or $S_aR_{S_a}^{0.5}$. The seismic demands are expressed in terms of a probabilistic hazard curve

(the annual probability of exceeding a specified intensity measure), determined either explicitly by a probabilistic seismic hazard analysis or using published hazard maps. Eq. (10) can be expanded into the following form using the total probability theorem:

$$P_f = \int_0^\infty H_{IM}(u)\, f_{\lambda_f}(u) du \tag{11}$$

where u is the intensity measure, $H_{IM}(u)$ is the hazard curve, and $f_{\lambda_f}(u)$ is the probability density of the structural stability limit. To permit closed-form solution of the probability integral, the hazard function is assumed to take the following form:

$$H_{IM}(u) = k_o u^{-k} \tag{12}$$

where k_o and k are coefficients that fit Eq. (12) to the hazard data. Further, $f_{\lambda_f}(u)$ is assumed as a lognormal distribution with the median $\hat{\mu}_{\lambda_f}$ and the dispersion $\delta_{\lambda f}$ (or $\sigma_{ln(\lambda f)}$). Given these assumptions, the integral solution to Eq. (11) is as follows:

$$P_f = H_{IM}(\hat{\mu}_{\lambda_f}) e^{\frac{1}{2}k^2\delta^2_{\lambda_f}} \tag{13}$$

where $H_{IM}(\hat{\mu}_{\lambda_f})$ is the mean annual probability from the hazard curve evaluated at the median capacity $\hat{\mu}_{\lambda_f}$, and the other terms are as defined previously.

6.2 LRFD-like Format of Collapse Probability

An alternative way to envision the mean annual collapse probability is by rearranging Eq. (13) so as to compare the hazard demand to the structural capacity in a format similar to that used for Load and Resistance Factor Design (LRFD) provisions. Setting the failure probability in Eq. (13) to a maximum acceptance probability criteria, $P_f < P_{acceptance}$, Eqs. (12 & 13) can be combined to give the design requirement:

$$k_o \hat{\mu}_{\lambda_f}^{-k} e^{\frac{1}{2}k^2\delta^2_{\lambda_f}} < P_{acceptance} \tag{14}$$

Rearranging this equation, the required capacity $\hat{\mu}_{\lambda_f}$ to ensure that the probability of failure is less than the acceptance criterion, $P_{acceptance}$, is given by the following:

$$\hat{\mu}_{\lambda_f} \geq IM_{P_{acceptance}} e^{\frac{1}{2}k\delta^2_{\lambda_f}} \tag{15}$$

where $IM_{P_{acceptance}}$ is the hazard intensity measure with the annual probability, $P_{acceptance}$, of being exceeded (i.e. $P_{acceptance} = H_{IM}(IM_{P_{acceptance}})$). The term, $e^{1/2 k\delta^2_{\lambda_f}}$, which reflects the variability of the median stability limit $\hat{\mu}_{\lambda_f}$, can be moved to the left side of Eq. (15), resulting in the following:

$$e^{-1/2 k\delta^2_{\lambda_f}} \hat{\mu}_{\lambda_f} \geq IM_{P_{acceptance}} \quad or \quad \phi \hat{\mu}_{\lambda_f} \geq \text{“}seismic\ demand\text{”} \tag{16}$$

where $\phi = e^{-1/2 k\delta^2_{\lambda_f}}$. This equation is similar to LRFD equations that are prevalent in code provisions where the “design strength” on the left side (the nominal strength reduced by a phi factor) is compared to the load effect or “seismic demand”. In this case there is no load factor on the seismic demand since the recurrence interval of the demand is implicit in its definition.

Essentially, Eq. (16) enables one to establish whether a structure meets the collapse performance objective with a mean annual probability of exceedance, $P_{acceptance}$. There are two basic input requirements for the procedure: (1) the “seismic demand” for the desired probability of exceedance, $IM_{Pacceptance}$, determined using either hazard maps or a probabilistic seismic hazard analysis; and (2) the median stability limit, $\hat{\mu}_{\lambda_f}$, of the structure and the corresponding dispersion, δ_{λ_f}, for a representative set of ground motions.

7. APPLICATION OF PROBABILISTIC COLLAPSE ASSESSMENT

This example will go through a collapse performance assessment for 6S_RCS_P frame. The hazard analysis is based on a site at Yerba Buena Island (in San Francisco Bay) where the San Andreas and Hayward faults govern the seismic hazard. The seismic hazard is characterized by two ways: (1) through an explicit probabilistic seismic hazard analysis of the site and (2) using spectral acceleration hazard maps from building code provisions.

7.1 Annual Hazard Curves

Probabilistic Seismic Hazard Analysis (PSHA): Using attenuation relationship in Eqs. (6 and 7), annual hazard curves for spectral acceleration, $S_a(T_1)$, and the proposed intensity measure, $S_a R_{S_a}{}^{0.5}$, are developed through a standard PSHA for the Yerba-Buena site. Details of the hazard analysis are beyond the scope of this paper.

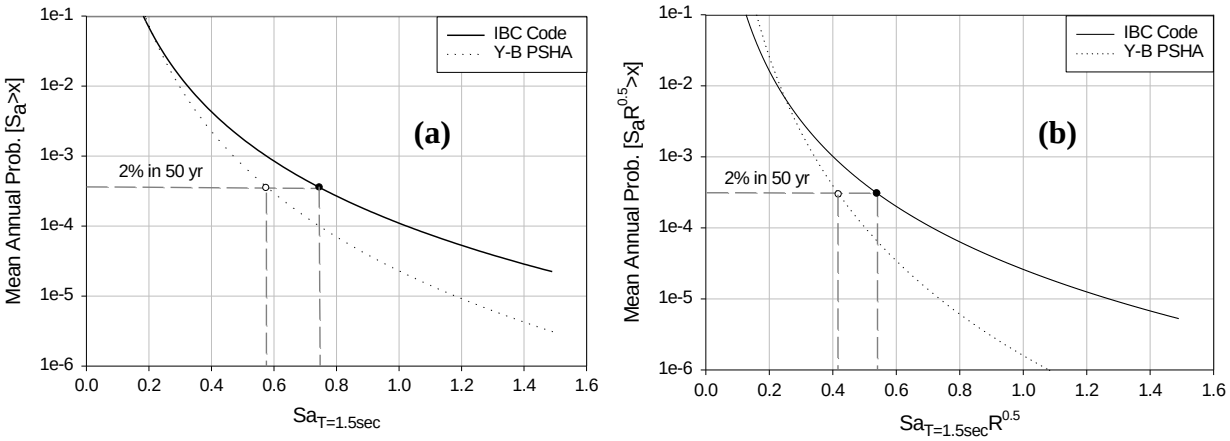

Fig. 8. Site Hazard Curves (a) S_a and (b) $S_aR^{0.5}$ (T_1 = 1.5 seconds).

Code Based Technique: An alternative (simplified) technique to obtain the hazard curve is to infer it from mapped spectral and site coefficients [1]. The first step is to calculate the spectral acceleration for the site using the following equation:

$$S_a = F_v S_1 / T_1 \tag{17}$$

where F_v is a tabulated site coefficient, given as a function of the site (soil) class and the spectral coefficients, and S_1 is the spectral hazard coefficient obtained from seismic hazard maps with an average probability of occurrence of 2% in 50-years. Implied by Eq. (17) is a 1/T spectral curve in the long period range. Using Eq. (17), one can directly obtain the 2% in 50 year (P_o = *0.0004*) spectral acceleration at the first mode period T_1, i.e., $S_a(T_1)$. One can also approximate the two-parameter index $S_a R_{S_a}{}^{0.5}$, by assuming that $R_{S_a} = 1/2 \quad \langle = S_a(2T_1)/S_a(T_1) = T_1/2T_1 \rangle$. Two approximations inherent in this assumption are that there is full correlation between the hazard values of $S_a(T_1)$ and $S_a(2T_1)$, and the *1/T* design spectrum accurately represents the hazard spectrum.

Once the 2% in 50 year spectral values are known, the full hazard curve is constructed assuming k = 4, and then back-calculating the k_o parameter, defined as per Eq. (12).

Hazard Curve Comparison: Hazard curves for $T_1 = 1.5$ seconds (the natural period for 6S_RCS_P frame) are shown in Fig. 8, and the corresponding hazard curve parameters are summarized in Table 2. Also summarized in Table 2 are capacity statistics $\hat{\mu}_{\lambda_f}$ and δ_{λ_f} for the frame. Referring to Fig. 8a, the 2% in 50 year value of $S_a(T_1)_{PSHA}$ = 0.56g from PSHA is about 20% less than the code-value of $S_a(T_1)_{Code}$ = 0.72g, and there are corresponding differences over the entire hazard curve. Presumably the PSHA results are more accurate, but further studies would need to be done to confirm this. Referring to Fig. 8b, the difference between the PSHA and code approach at the 2% in 50 year level for the S_aR_{sa} index is also about 20%, $S_a(T_1)R_{Sa\ PSHA}^{0.5}$= 0.40 versus $S_a(T_1)R_{Sa\ Code}^{0.5}$= 0.51g.

Table 2. Hazard curve coefficients and mean and dispersion of capacity

IM	Yerba Buena Site		Code Based Technique		$\hat{\mu}_{\lambda_f}$	δ_{λ_f}
	k_o	k	k_o	k		
$S_a(T_1)$	$2.3\text{x}10^{-5}$	5.0	$1.1\text{x}10^{-4}$	4	1.45	0.31
$S_aR_{Sa}^{0.5}$	$1.6\text{x}10^{-6}$	6.0	$2.6\text{x}10^{-5}$	4	0.76	0.15

7.2 Probability of Failure

Summarized in Table 2 are all the necessary data to compute the mean annual failure probabilities for 6S_RCS_P frame using the two alternative hazard intensity measures, $S_a(T_1)$ and $S_a(T_1)R_{Sa}^{0.5}$, and two alternative hazard curves (PSHA and building code approach). Substituting this data into Eqs. (12 and 13), the resulting collapse probabilities, P_f, are calculated and summarized in Table 3.

For the code hazard spectra and the $S_a(T_1)$ index, the mean annual probability of exceeding the stability (collapse) performance is about 0.00005 or roughly a 0.3% chance of exceedance in 50 years. Using the $S_aR_{S_a}^{0.5}$ index the probability roughly doubles to a mean annual value of 0.00009 or roughly a 0.5% in 50-year level. Since

these probabilities are less than one-fourth of the 2% in 50-year seismic hazard probability commonly used as the target for collapse prevention performance, this data suggests that current code provisions result in a conservative design for this case. Moreover, the failure probabilities are less by about a factor of five using the PSHA intensity data, implying an additional degree of conservatism in the design.

Table 3. Failure probability and capacity factor design factors

		Yerba Buena Site	Code Based Technique
Probability of Failure	$P_f(S_a(T_1))$	1.19×10^{-5}	5.37×10^{-5}
	$P_f(S_a R_{Sa}^{0.5})$	1.24×10^{-5}	9.29×10^{-5}
$IM = S_a(T_1)$	ϕ	0.78	0.82
	$\phi\mu_{\lambda f}$	1.13g	1.19g
	10%in50year	0.41g	0.48g
	2%in50year	0.56g	0.72g
$IM = S_a R_{S_a}^{0.5}$	ϕ	0.94	0.96
	$\phi\mu_{\lambda f}$	0.72g	0.73g
	10%in50year	0.30g	0.34g
	2%in50year	0.40g	0.51g

Concerning the different results obtained using the $S_a(T_1)$ versus $S_a R_{S_a}^{0.5}$ index, the fact that the two-parameter index results in higher failure probabilities suggests that for predicting collapse performance, simple scaling based on $S_a(T_1)$ may be unconservative. This follows from the logic that the two-parameter index more accurately represents the damaging effects of earthquakes in the hazard curve. Note, however, that the difference between the two indices is not too large for the Yerba Buena site analysis (PSHA) where the correlation between $S_a(T_1)$ and $S_a(T_f)$ is modeled more accurately than in the code-based technique.

7.3 Factored Capacity versus Nominal Demand

An alternate way of assessing the analysis results is through the LRFD-like approach described by Eq. (16). Data for this method are summarized in the lower half of Table 3, where limiting values are reported for 2% in 50-year (0.0004) and 10% in 50-year (0.002) probability levels. Referring to Table 3, the ϕ factor ranges from

$\phi = 0.78$ to 0.82 for the $S_a(T_1)$ index and from $\phi = 0.94$ to 0.96 for the $S_a R_{S_a}{}^{0.5}$ index. The large difference between these ranges is directly related to the reduced dispersion achieved using the two-parameter $S_a R_{S_a}{}^{0.5}$ index as compared to the $S_a(T_1)$ index.

According to the criteria, $\phi \hat{\mu}_{\lambda_f} \geq IM_{P_{acceptance}}$, the frame collapse performance limit passes the 2% in 50-year and 10% in 50-year probability checks in all cases. These comparisons do reflect the relative difference in results between the $S_a(T_1)$ and $S_a R_{S_a}{}^{0.5}$ indices that is similar to the difference observed in the failure probabilities described previously. For example, consider the ratio $\phi \hat{\mu}_{\lambda_f} / IM_{P_{acceptance}}$ between the factored capacity and the hazard intensity. Using data from the Yerba-Buena PSHA at the 2% in 50-year level, the ratios are $\phi \hat{\mu}_{\lambda_f} / Sa_{2\%in50}$ = 1.13/0.56 = 2.0 for the $S_a(T_1)$ index and $\phi \hat{\mu}_{\lambda_f} / SaR_{Sa2\%in50}$ = 0.72/0.4 = 1.8 for the $S_a R_{S_a}{}^{0.5}$ index.

8. SUMMARY AND CONCLUSIONS

A method to assess seismic response and probabilistic collapse performance of structures is presented and demonstrated by application to moment frame buildings. Included is a proposal for a new two-parameter earthquake hazard intensity measure $S_a R_{S_a}{}^{0.5}$ that reflects both spectral intensity and spectral shape, thus accounting for inelastic strength and stiffness degradation (period elongation). Data presented shows that this proposed index significantly reduces the record-to-record variability in predicted response obtained from inelastic time history analyses. This has practical implications on improving the accuracy of seismic assessment methods and reducing the number of records necessary to obtain a given confidence in the results.

Equations are also developed to interpret the probability of collapse using data from incremented dynamic analyses. The equations are presented in two formats, one that directly computes the probability of failure for a structure, and another, which mimics an LRFD format by applying a “phi-factor” to the capacity of the structure and comparing it to a specified hazard.

REFERENCES

1. ICC, “International Building Code”, International Code Council, contact: BOCA, Country Club Hills, IL, 2000.
2. Housner, G. W., “Measures of Severity of Earthquake Ground Shaking”, Proc. of the U.S. Nat. Conf. on Earthquake Engrg, EERI, Oakland, CA, pgs 25-33, 1975.
3. Luco, N., "Probabilistic Seismic Demand Analysis, SMRF Connection Fractures, and Near-Source Effects", Ph.D. Thesis, Stanford Univ., Stanford, CA, 2001.
4. Alavi, B., and Krawinkler, H., “Consideration of Near-Fault Ground Motion Effects in Seismic Design”, Proc. of 12th World Conf. on Earthquake Engrg., New Zealand, 8 pg., 2000.
5. Inoue, T., “Seismic Hazard Analysis of Multi-degree-of-freedom Structures”, Report No. RMS-8, Stanford University, Stanford, CA, 1990.
6. Abrahamson, N.A., and Silva, W.J., “Empirical Response Spectral Attenuation Relations for Shallow Crustal Earthquakes”, Seismological Research Letters, 68(1), 94-127, 1997.
7. Mehanny, S.S., and Deierlein, G.G., “Modeling and Assessment of Seismic Performance of Composite Frames with Reinforced Concrete Columns and Steel Beams”, J.A. Blume Earthquake Engrg. Center, Tech. Rep. No. 135, Stanford, CA, 2000.
8. El-Tawil, S., and Deierlein, G.G., “Inelastic Dynamic Analysis of Mixed Steel-Concrete Space Frames”, Struct. Engrg. Rep. No. 96-5, Cornell Univ., Ithaca, NY, 1996.
9. Shome, N., and Cornell, C.A., “Probabilistic Seismic Demand Analysis of Nonlinear Structures,” Rep. No. RMS-35, Stanford Univ., Stanford, CA, 1997.

استنباط مقياس ثنائى المقدار للشدة الزلزالية وطريقة لتقييم التصميم بالاحتمالات

يتناول البحث طريقة لتقييم الانهيار فى الإطارات تحت تأثير الزلازل آخذاً فى الاعتبار عدم دقة المعلومات فى كل من الحركة الأرضية والتصرف اللدن للمنشآت، وتشمل الطريقة استنباط معاير جديد لقياس الشدة الزلزالية يحتوى على الاستطالة فى زمن الذبذبة الاساسى وبالتالى يقلل التباين الملحوظ فى التصرف اللدن للمنشآت عند استخدام التحليل الإنشائى المعتمد على الزمن تحت تأثير زلازل مختلفة لها نفس مقياس الشدة، كما تم استنتاج بعض المعادلات الرياضية التى تستخدم نتائج التحليل اللدن المعتمد على الزمن مع منحنى الخطورة الزلزالية الخاص بموقع ما لحساب الاحتمال السنوى المتوسط لمنشأ حتى يصل الى حالة الانهيار.